STARD4 knockdown in HepG2 cells disrupts cholesterol trafficking associated with the plasma membrane, ER, and ERC

Jeanne Garbarino,* Meihui Pan,* Harvey F. Chin,† Frederik W. Lund,†,§ Frederick R. Maxfield,† and Jan L. Breslow[1],*

The Laboratory of Biochemical Genetics and Metabolism,* The Rockefeller University, New York, NY 10065; and Department of Biochemistry,† Weill Medical College of Cornell University, New York, NY 10065; and Department of Biochemistry and Molecular Biology,§ University of Southern Denmark, DK-5230 Odense M, Denmark

Abstract STARD4, a member of the evolutionarily conserved START gene family, has been implicated in the nonvesicular intracellular transport of cholesterol. However, the direction of transport and the membranes with which this protein interacts are not clear. We present studies of STARD4 function using small hairpin RNA knockdown technology to reduce STARD4 expression in HepG2 cells. In a cholesterol-poor environment, we found that a reduction in STARD4 expression leads to retention of cholesterol at the plasma membrane, reduction of endoplasmic reticulum-associated cholesterol, and decreased ACAT synthesized cholesteryl esters. Furthermore, D4 KD cells exhibited a reduced rate of sterol transport to the endocytic recycling compartment after cholesterol repletion. Although these cells displayed normal endocytic trafficking in cholesterol-poor and replete conditions, cell surface low density lipoprotein receptor (LDLR) levels were increased and decreased, respectively. We also observed a decrease in NPC1 protein expression, suggesting the induction of compensatory pathways to maintain cholesterol balance. These data indicate a role for STARD4 in nonvesicular transport of cholesterol from the plasma membrane and the endocytic recycling compartment to the endoplasmic reticulum and perhaps other intracellular compartments as well.—Garbarino, J., M. Pan, H. F. Chin, F. W. Lund, F. R. Maxfield, and J. L. Breslow. **STARD4 knockdown in HepG2 cells disrupts cholesterol trafficking associated with the plasma membrane, ER, and ERC. *J. Lipid Res.* 2012.** 53: **2716–2725.**

Supplementary key words cholesterol • StAR-related lipid transfer domain protein • hepatocellular carcinoma • intracellular cholesterol transport • endoplasmic reticulum • endocytic recycling compartment • low density lipoprotein receptor

The asymmetric distribution of free cholesterol (FC) within the endomembrane system makes apparent the high level of regulation associated with intracellular cholesterol transport. For example, the endoplasmic reticulum (ER) has very low levels of FC (0.1% to 2% of total cellular FC), whereas the plasma membrane (PM), which has similar surface area to the ER, contains 65% to 80% of total cellular FC (1). The precise mechanism responsible for this intracellular cholesterol gradient is not well understood, but it is likely achieved through the concerted efforts of a number of different homeostatic mechanisms, including tightly controlled transport processes.

Both vesicular transport, an ATP-dependent process requiring an intact cytoskeleton, and nonvesicular transport, which involves carrier proteins and occurs independent of ATP, have been implicated in intracellular cholesterol movement (2). Examples of the latter include experiments treating macrophages and fibroblasts with sphingomyelinase, which triggers the release of cholesterol from the PM to the ER, resulting in ACAT-mediated cholesterol esterification (3, 4). This occurs, albeit at a reduced rate, even under conditions of ATP depletion or in the presence of vesicular trafficking inhibitors, implicating nonvesicular pathways in the transport of cholesterol (5). Furthermore, cholesterol is transported to mitochondria, which are not directly connected to the vesicular cholesterol transport network, to serve as the starting material for the synthesis of steroid hormones (6–8). These and other observations suggest that nonvesicular cholesterol transport proteins play a key role in maintaining intracellular cholesterol homeostasis.

This work was supported by National Institutes of Health grants HL007824 and R37-DK27083. Its contents are solely the responsibility of the authors and do not necessarily represent the official views of the National Institutes of Health or other granting agencies. F.W.L. acknowledges funding from the Danish Research Council for Health and Disease given to his PhD advisor Dr. Daniel Wüstner (grant no. 23569).

Manuscript received 14 September 2012 and in revised form 1 October 2012.

Published, JLR Papers in Press, October 2, 2012
DOI 10.1194/jlr.M032227

Abbreviations: CE, cholesteryl ester; DHE, dehydroergosterol; ER, endoplasmic reticulum; ERC, endocytic recycling compartment; FC, free cholesterol; FRAP, fluorescence recovery after photobleaching; LDLR, low density lipoprotein receptor; LPDS, lipoprotein-deficient serum; NPC, Niemann Pick Type C; PM, plasma membrane; shRNA, small hairpin RNA; START, StAR-related lipid transfer; Tf, transferrin; TfR, transferrin receptor.

[1]To whom correspondence should be addressed
e-mail: breslow@rockefeller.edu

Copyright © 2012 by the American Society for Biochemistry and Molecular Biology, Inc.

This article is available online at http://www.jlr.org

Several proteins with the capacity to bind cholesterol have been implicated in the intracellular movement of cholesterol, including Niemann Pick Type C proteins (NPC1 and NPC2), oxysterol binding proteins, sterol carrier protein 2, caveolins, and StAR-related lipid transfer (START) proteins (9, 10). Proteins belonging to the START family, which include the well-documented intracellular cholesterol transporters StAR and MLN64 (11), are defined by a 200–230 amino acid domain organized as a helix-grip fold forming a hydrophobic cavity that can accommodate a lipid molecule. The architecture of the START domain determines the specificity of the lipid ligand (7, 12), and both StAR and MLN64 bind and transport cholesterol for use during steroidogenesis (10) and intracellular cholesterol trafficking from endosomes (13), respectively.

An additional member of the START protein gene family, STARD4, binds and transports FC within cells based on several lines of evidence, including in vitro binding studies (14) and sequence homology to the START domains of known cholesterol transporters StAR and MLN64 (15). Furthermore, the X-ray crystal structure of mouse STARD4 indicates that its START domain forms a hydrophobic pocket capable of binding one molecule of FC (16). In addition, it has been shown that STARD4 expression is regulated by cholesterol through the transcription factor SREBP2.

Based on cell culture models of over expression, it has been hypothesized that STARD4 transports cholesterol to or from the ER. Strengthening this STARD4-ER relationship is supported by the observation of enhanced in vitro ACAT activity by addition of recombinant STARD4 protein to isolated microsomes. Additional in vitro studies have suggested that STARD4 is capable of delivering cholesterol to isolated mitochondria, presumably to provide substrate for the alternate bile acid synthesis pathway (14, 17, 18). Although current research suggests interactions between STARD4 and specific organelles, such as the ER and mitochondria, the membranous source of FC, as well as any net directionality of STARD4-mediated cholesterol transport, need clarification and are the goals of this study.

Due to the importance of the liver in whole-body cholesterol homeostasis, we used the human hepatoma cell line, HepG2, as a model to examine STARD4 function. We created stable HepG2 StarD4 knockdown cells (D4 KD) using lentiviral small hairpin RNA (shRNA) technology and in cholesterol-poor conditions showed that these cells had retention of cholesterol at the PM, reduction of ER-associated cholesterol, and decreased ACAT-synthesized cholesteryl esters. Furthermore, after a short period of cholesterol repletion in the presence of the fluorescent cholesterol analog dehydroergosterol (DHE), we showed that D4 KD cells exhibited a reduced rate of fluorescent recovery after photobleaching (FRAP) at the endocytic recycling compartment (ERC). Additionally, in cholesterol-poor and cholesterol-replete conditions, D4 KD cells showed normal trafficking of transferrin (Tf) and its receptor (TfR). Yet, relative to control cells, D4 KD cells had increased LDLR at the cell surface under cholesterol-poor conditions, whereas cholesterol repletion resulted in decreased LDLR at the cell surface relative to control cells. These data provide evidence that STARD4 is associated with the plasma membrane, ER and the ERC, and disruptions in STARD4 function induces compensatory pathways to maintain cholesterol homeostasis.

MATERIALS AND METHODS

Cell culture and treatments

HepG2 cells (ATCC) were maintained on collagen-coated plates in MEM (Invitrogen) supplemented with 10% FBS (Sigma Aldrich) and 1× penicillin/streptomycin (Invitrogen) at 37°C and 5% CO_2. On the day before each experiment, cells were washed twice with PBS, and the media was replaced with MEM supplemented with 5% lipoprotein-deficient serum (LPDS) (Intracel) and 1× penicillin/streptomycin and incubated for 20 h. Cholesterol loading was performed using a methyl-β-cyclodextrin:cholesterol (6.5:1) complex for 90 min as described (17).

RNA isolation and qRT-PCR

Total RNA was isolated from HepG2 cells using Trizol (Invitrogen) according to the manufacturer's specifications. Total RNA (1 μg) was used for cDNA synthesis using Superscript III First Strand cDNA Synthesis Kit (Invitrogen). For qRT-PCR, SYBR Green (Applied Biosystems) was used to amplify ~2 ng of cDNA using an Applied Biosystems 7900 apparatus. Absolute copy number was determined based on standard curve values, and relative quantification was performed using ΔCT. β-Actin was used as a housekeeping gene for all experiments. Analysis was performed on at least three independent RNA isolations per cell line and/or condition.

Generation of stable STARD4 knockdown cell lines using lentiviral shRNA transduction

The shRNA Lentiviral Delivery System was obtained from Dharmacon, and transduction was performed according to the manufacturer's specifications. Briefly, HepG2 cells were seeded onto collagen-coated 96-well plates at a density of 25,000 cells per well. On the following day, lentiviral particles containing a specific sequence against STARD4 or a nontargeting control sequence were transduced into HepG2 cells. The number of lentiviral particles for this knockdown experiment was determined in previous titration pilot studies, where it was determined that a multiplicity of infection of 40 would be most effective. Stably transduced cells were selected by culturing in the presence of puromycin (1 μg/ml) for several days.

Fluorescence microscopy

HepG2 cells were grown on collagen-coated cover slips for all imaging experiments. Staining with filipin reagent (Sigma Aldrich) was performed as described (19). Briefly, cells were washed three times with Medium 1 (150 mM NaCl, 5 mM KCl, 1 mM CaCl2, 20 mM HEPES [pH 7.4], 2 mg/ml glucose) and fixed in 4% paraformaldehyde solution for 20 min at room temperature. Cells were washed with PBS followed by incubation with 50 μg/ml of Filipin in Medium 1 for 2 h in the dark. Cells were washed three times with Medium 1, and cover slips were mounted onto slides using VectaSheild mounting solution (Vector Laboratories, Inc.). Cells were imaged on an Olympus IX-70 deconvolution inverted microscope using a 60× objective. The excitation/emission spectrum for fIlipin/cholesterol complexes was 340/420. Images were captured with a Hamamatsu camera and analyzed using Deltavision software.

LC-MS for the determination of cholesterol mass

HepG2 cell lines were grown on collagen-coated 6-well plates (in triplicate) until approximately 80% confluent. Media was aspirated, and cells were washed twice with PBS. Cells were then provided with MEM containing 5% LPDS and antibiotics and cultured at 37°C and 5% CO_2 for 20 h. After LPDS pretreatment, the cells were washed twice with PBS, and lipids were extracted u sing hexane:isopropanol (3:2 v/v) containing β-sitosterol as an internal standard such that the final concentration of β-sitosterol was 5 μg per sample. Lipid extracts were transferred to borosilicate tubes. Two thirds of the lipid extract from each sample was transferred to a fresh borosilicate tube and used for the determination of total cholesterol amounts. These extracts were dried under nitrogen gas and subjected to a chemical hydrolysis reaction to liberate esterified cholesterol by adding MeOH containing 3.3% KOH and heating to 80°C for 1 h. Tubes were allowed to equilibrate to room temperature, and a water:hexane mixture (1.5:2.5 v/v) mixture was added. Each sample was vortexed for 1 min, and, after a 3 min centrifugation at 1,000 rpm, the top layer was transferred to a fresh tube and dried under nitrogen gas. The remaining one third of the lipid extracts were dried under nitrogen gas and used to determine FC levels. All samples were resuspended in hexane, and lipids were separated using a Varian Factor Four capillary column (VF-1 ms 30 m × 0.25 mm ID DF 0.25) using Varian 4000 GC/MS/MS system. Total cholesterol and FC values were determined and normalized to total protein. Cholesteryl ester (CE) levels were determined by subtracting FC amounts from total cholesterol.

Fluorescence recovery after photobleaching

Fluorescence recovery after photobleaching (FRAP) experiments were carried out using a Leica DMIRB microscope equipped with an Andor iXonEM Blue EMCCD camera driven by MetaMorph Imaging System software (Universal Imaging/Molecular Devices, Sunnyvale, CA). Images were acquired using a 100× oil-immersion objective with 2 × 2 pixel binning. Cells being imaged were colabeled with DHE incubated with 10 μg/ml Alexa 633-Tf for 1 h at 37°C in Medium A/glucose (150 mM NaCl, 20 mM HEPES [pH 7.55], 1 mM CaCl2, 5 mM KCl, 1 mM MgCl2, 2 mg/ml glucose) to identify the ERC. DHE was imaged using a filter cube obtained from Chroma Technology Corp. (Bellows Falls, VT) (335 nm [20 nm band pass] excitation filter, 365 nm long pass dichromatic filter, and 405 nm [40 nm band pass] emission filter). Transferrin was imaged with a standard TRITC cube obtained from Chroma. A prebleach image was acquired before bleaching. DHE in the ERC was photobleached, and images were taken every 30 s. The fluorescence intensity ratio of the photobleached area (ERC) to the entire cell was calculated for each time point and normalized using prebleach (100%) and t = 0 (0%) images. The recovery curves were fitted to determine the half time of recovery using SigmaPlot (Systat Software Inc., San Jose, CA). The recovery curves were fitted by (20):

$$F(t) = \frac{F(0) + F(\infty)(t/t_{½})}{1 + (t/t_{½})}$$

where $F(0)$ and $F(\infty)$ are the fluorescence intensities at time t = 0 and at full recovery, respectively, and $t_{1/2}$ is the half time of recovery.

Tf recycling rates

Control or STARD4 knockdown HepG2 cells were cholesterol loaded for 1.5 h with 0.5 mM MBCD-cholesterol before labeling with Alexa555-transferrin for 1 h. Labeled Tf was chased with excess unlabeled Tf in the presence of 20 μM deferoxamine and fixed at the indicated time points. Cells were imaged as described above, and fluorescence intensity was measured for individual cells in multiple fields (n > 50 cells for each point).

Subcellular membrane fractionation

HepG2 cell lines were grown on collagen-coated 150 cm plates (5 per cell line or condition) until approximately 80% confluent. Media was aspirated, and cells were washed twice with PBS. Cells were then provided with MEM containing 5% LPDS and antibiotics and cultured at 37°C and 5% CO_2 for 20–24 h. For subcellular membrane fractionation, cells were placed on ice and washed twice with ice-cold PBS. Cells were scraped in cold Solution A (0.25 M sucrose, 1 mM EDTA, 10 mM HEPES [pH 7.4], Roche Complete mini Protease inhibitor tablet). Cells were homogenized by passing through a 23 guage syringe 15–20 times. Homogenate was spun at 3,000 *g* for 10 min at 4°C, and the supernatant was transferred to a fresh tube. The pellet was resuspended in Solution A, and homogenization was repeated. Supernatants were combined and loaded on top of a discontinuous 2.5–30% OptiPrep (Axis-Shield) gradient and spun at 41,000 rpm for 2.5 h at 4°C using an SW 41.T rotor. Fractions were collected in 1 ml increments and used for cholesterol mass analysis using the Amplex Red Cholesterol Assay Kit (Invitrogen) and immunoblotting for specific markers.

Protein isolation and immunoblotting

Protein was isolated from HepG2 cell lines using a CHAPS Lysis Buffer (40 mM HEPES [pH 7.5], 120 mM NaCl, 1 mM EDTA, 0.3% CHAPS, protease and phosphatase inhibitors) and quantified using a BCA assay kit (Pierce). Total protein (30 μg) was subjected to SDS-PAGE and transferred onto nitrocellulose membranes. For immunoblotting, membranes were blocked in PBST containing 5% nonfat milk followed by primary antibody incubation in PBST containing 5% BSA at 4°C over night. Membranes were washed three times for 5 min in PBST followed by incubation in the appropriate secondary antibody (HRP conjugated) diluted in PBST containing 5% BSA for 1–2 h at room temperature. Membranes were washed three times for 5 min in PBST, and signal was detected using SuperSignal West Pico Chemiluminescent Substrate (Pierce) and exposed to film. GM130 was from Abcam; LDLR and STARD5 were from Novus Biologicals; OSBP was from Proteintech; STARD4 was from Santa Cruz Biotechnology; SCP-2, NPC1, and FABP1 were from Sigma; and TfR was from Invitrogen. All other antibodies were from Cell Signaling Technology.

ACAT activity assay

^{14}C-oleate (Perkin Elmer) was conjugated to albumin as described (21). HepG2 cell lines were grown in triplicate on collagen-coated 6-well plates until approximately 80% confluent. Media was aspirated, and cells were washed twice with PBS. Cells were then provided with MEM containing 5% LPDS and antibiotics and cultured at 37°C and 5% CO_2 for 20 h. Compactin (100 nM) was also added with LPDS media. Experimental cells were pretreated with the ACAT inhibitor F1394 (2μM) for 2 h followed by the addition of ^{14}C-oleate-albumin for 1 h. Cells were washed three times with PBS followed by lipid extraction using hexane:-isopropanol (3:2, v/v). After drying organic extracts under N_2, lipids were reconstituted in chloroform methanol (2:1) and spotted onto silica coated glass TLC plates. Lipids were resolved in petroleum ether:diethyl ether:acetic acid (85:14:1, v/v). Lipid species were visualized by exposing to iodine vapor, and levels of radioactive incorporation into cholesteryl ester was quantified through scintillation spectroscopy. Protein was extracted from delipidated cells using 0.1 N NaOH and measured using the BCA assay. Lipid values were normalized to total protein.

Biotinylation of cells surface proteins

Confluent control and D4 KD cells were grown for 20 h in media supplemented with 5% LPDS, and cell surface proteins were biotinylated using the Pierce Cell Surface Protein Isolation Kit (ThermoFisher) according to the manufacturer's specifications. The biotinylated proteins were subjected to SDS-PAGE, and the amount of biotinylated TfR and LDLR was determined by immunoblotting.

Statistical analysis

A minimum of three replicates per cell line or condition were used for each experiment, and each experiment was independently confirmed in triplicate. In the instance of quantification, standard deviations, unless otherwise stated, were calculated, and *P* values were determined using a *t*-test and a 95% confidence interval.

RESULTS

STARD4 expression in HepG2 cells cultured in lipoprotein-deficient media

To develop a model system to study STARD4 function, we set out to uncover the condition under which STARD4 expression is maximized in vivo. Previous studies in other cell types have shown that cholesterol down-regulates STARD4 expression via the transcription factor SREBP2 (15, 22). Based on these results, we hypothesized that STARD4 expression would be induced in HepG2 cells under conditions of cholesterol deficiency. To test this, we adopted a protocol used by Brown and Goldstein in their seminal 1973 paper describing 3-hydroxy-3-methylglutaryl coenzyme A reductase regulation in fibroblasts from normal subjects and patients with heterozygous and homozygous familial hypercholesterolemia (23, 24).

The response of STARD4 to cholesterol deficiency was examined in HepG2 cells cultured for 20 h in medium containing 5% lipoprotein-deficient serum (LPDS), compared with 10% FBS. As expected, STARD4 is clearly induced at the mRNA (**Fig. 1A**) and protein levels (Fig. 1B) in HepG2 cells cultured in 5% LPDS. This confirmation helps to clearly define a specific response for STARD4, thereby providing the basis for a model system to examine certain aspects of STARD4 physiology.

Generation of stable STARD4 knockdown HepG2 cells

As shown in Fig. 1, we were able to define a condition under which STARD4 is maximally expressed in normal HepG2 cells. To uncover clues into STARD4 function, we examined the effects of reduced STARD4 expression under these same conditions. Stably transduced D4 KD and nontargeting control cells were generated using lentiviral-mediated shRNA knockdown technology as described in Materials and Methods. After reaching subconfluency in 10% FBS, D4 KD and control cells were switched to 5% LPDS for 20 h, and STARD4 expression was assessed. STARD4 levels in D4 KD cells reached only 40% of both the mRNA and protein levels achieved by control cells (**Fig. 2A, B**).

Cholesterol content and distribution is altered in D4 KD cells

After 20 h in 5% LPDS, D4 KD and control cells did not differ in total cholesterol and FC levels as measured by LC-MS. However, D4 KD cells displayed a 58% reduction in CEs ($P = 0.02$) (**Fig. 3A**). Although this effect on cholesterol esterification points to an interaction between STARD4 and the ER, it was not clear how the genetic manipulation of STARD4 affected the overall cellular cholesterol distribution because total cellular FC levels were unchanged.

To examine this more closely, we monitored cellular FC distribution using the polyene antibiotic filipin, a fluorescent compound that specifically binds FC. As shown in Fig. 3B, control cells exhibited a largely internalized filipin signal, whereas in D4 KD cells a majority of the filipin signal was located at the cell periphery, suggesting FC retention at the PM. This phenotype was largely maintained even under conditions of cholesterol repletion (LPDS + 500 μM Cho:CD). Although qualitative, these results are compatible with a role for STARD4 in delivering FC from the PM to internal membranes, including the ER, during cholesterol deficiency.

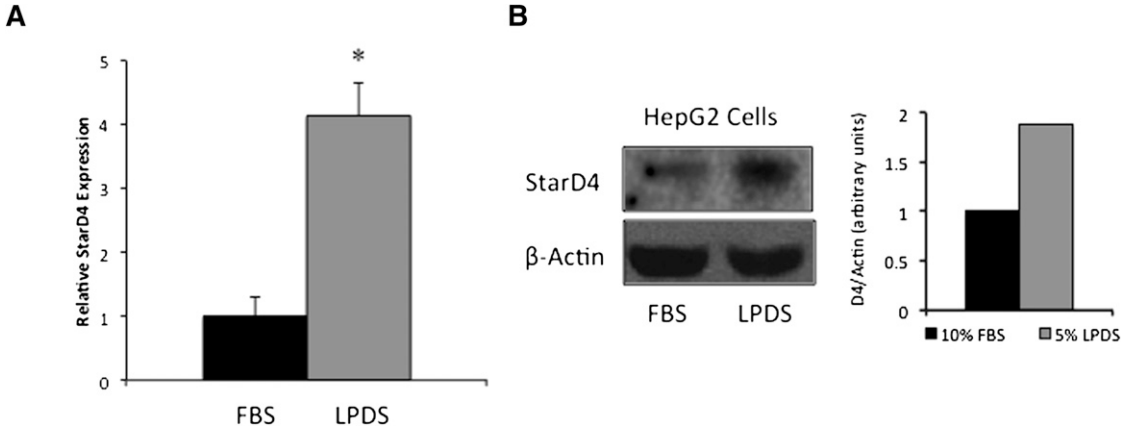

Fig. 1. STARD4 expression is up-regulated in response to growth in 5% LPDS. mRNA (A) and protein (B) levels in HepG2 cells were assessed after cells had been grown in medium containing 10% FBS or 5% LPDS for 24 h. The bar graph in panel B is a densitometric quantification of the immunoblot signal.

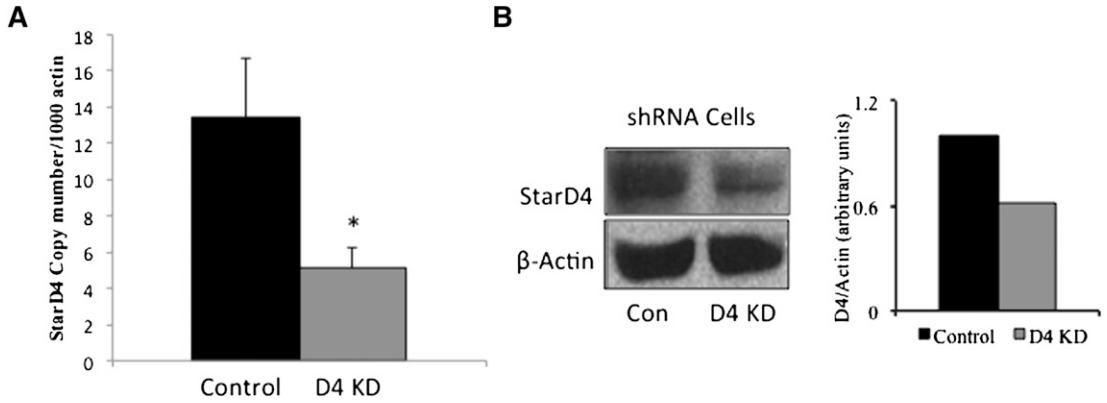

Fig. 2. STARD4 expression is reduced in response to STARD4 shRNA transduction. mRNA (A) and protein (B) levels in HepG2 cells were determined after 20 h in 5% LPDS. Control cell lines (Con) were transduced with a nontargeting sequence, whereas D4 KD cells were transduced with an shRNA sequence complimentary to human STARD4. The bar graph in panel B is a densitometric quantification of the immunoblot signal.

STARD4 knockdown results in decreased ACAT activity

The observations that D4 KD cells, under conditions of cholesterol deficiency, display reduced CE mass and retention of FC at the PM suggested that there was a decrease in the delivery of FC from the PM to the ER. It has been previously shown that STARD4 affects ACAT activity in cultured cells and in microsomes isolated from mouse livers (14). Together, these data led us to hypothesize that D4 KD cells also exhibited decreased ER-associated cholesterol esterification (ACAT activity) during cholesterol deficiency.

This was examined by culturing D4 KD and control cells for 20 h in 5% LPDS supplemented with 100 nM compactin. The latter, an HMG-CoA-reductase inhibitor, was used to block the contribution of endogenous cholesterol synthesis to the ER-associated cholesterol pool. A 1 h pulse with [^{14}C] oleate-albumin was used to assess ACAT activity

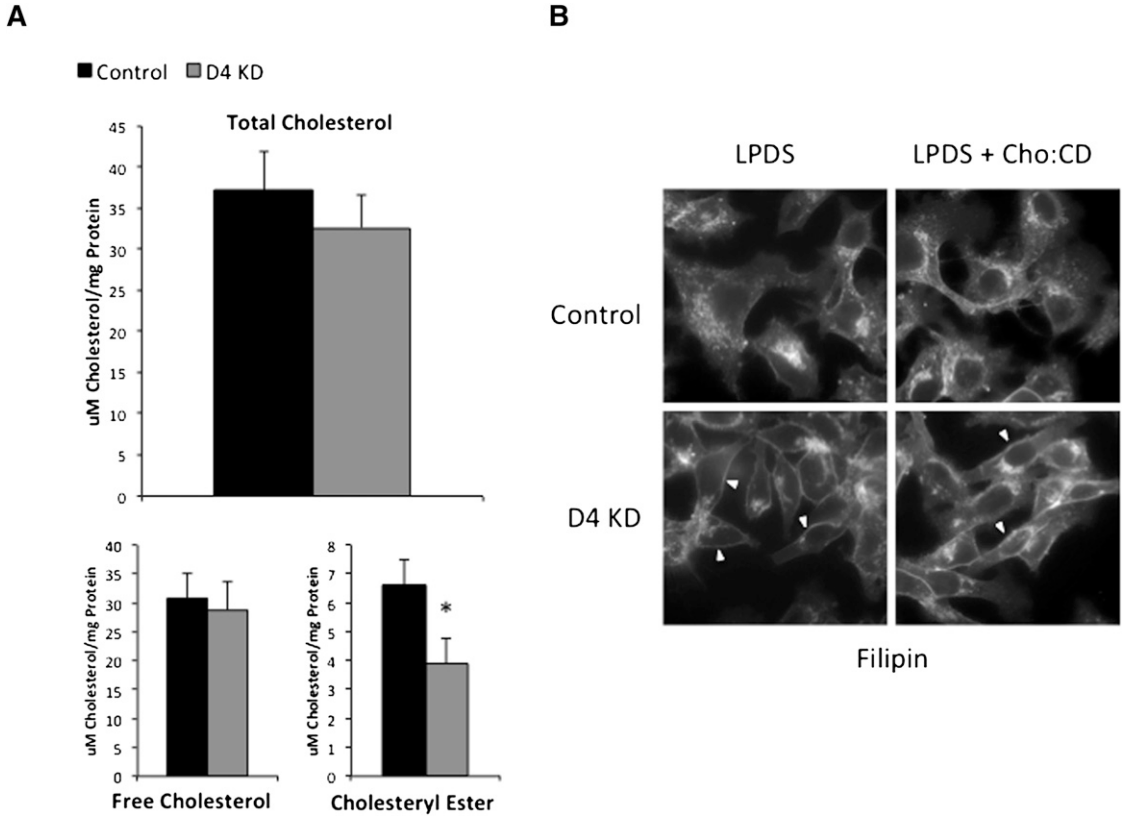

Fig. 3. Cholesterol mass and distribution in D4 KD cells after 20 h in 5% LPDS. A: Total, free, and esterified cholesterol levels in whole cell extracts were determined in control and D4 KD cells using LC-MS. B: The distribution of free cholesterol in control and D4 KD cells was determined using the fluorescent dye filipin under cholesterol-poor (LPDS) and cholesterol-replete (LPDS + 500 μM Cho:CD) conditions. Arrowheads in the D4 KD panel show areas of cholesterol retention at the cell periphery.

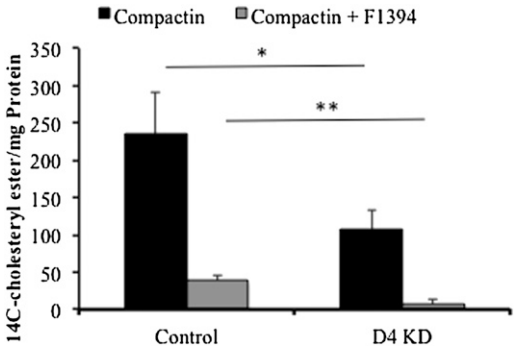

Fig. 4. ER-associated ACAT activity is diminished in D4 KD cells. The ACAT activity in control and D4 KD cells was assessed based on the incorporation of [^{14}C]oleate-albumin in the absence (black bars) or presence (gray bars) of the ACAT inhibitor F1394. The values represent the amount of radioactivity (CPM) specifically associated with cholesteryl esters, normalized to total cellular protein amounts.

and **Fig. 4** shows that ACAT activity was reduced by approximately 60% in D4 KD cells. Replicate incubations were undertaken in the presence of the ACAT-specific inhibitor F1394 (provided by Dr. Edward Fisher), which confirmed that most of the esterification observed was due to ACAT and not another ER-independent esterification reaction. Thus, D4 KD cells, when cultured under conditions of cholesterol deficiency, have reduced CE mass, diminished intracellular filipin signal, and decreased ACAT activity.

FC levels are decreased in subcellular membrane fractions corresponding to the ER

The decrease in ACAT activity in D4 KD cells under the condition of cholesterol deficiency led us to hypothesize that these cells have a diminished pool of ER-associated cholesterol. To test this, D4 KD and control cells were cultured for 20 h in 5% LPDS, and subcellular membrane fractionation was performed (25). The cells were mechanically lysed and layered onto a discontinuous OptiPrep gradient. After ultracentrifugation, 13 × 1 ml fractions were taken, and each fraction was assayed for cholesterol and membrane origin, the latter via immunoblotting with antibodies to specific membrane markers (ER-calnexin, Golgi-GM130, and early endosomes-EEA1). As shown in **Fig. 5A**, fractions 11–13 were ER enriched and relatively Golgi and endosome poor. Furthermore, these fractions isolated from D4 KD cells had about 70% less cholesterol than the same fractions from control cells (Fig. 5B). These results, in addition to reduced ACAT activity and diminished CE mass in the context of STARD4 deficiency in HepG2 cells, suggests that STARD4 delivers FC to the ER.

The rate of DHE fluorescent recovery at the ERC is diminished in D4 KD under cholesterol-replete conditions

One of the basic tenets of cell biology is the notion that FC is enriched in the PM of cells. Similarly, it has been reported that the ERC is also enriched in FC because it rapidly equilibrates with the FC pool in the PM (26). However, the ERC is not merely a storage depot, and the movement of cholesterol to and from this organelle is a very dynamic process. Several lines of evidence suggests that cholesterol transport to and from the ERC occurs through mainly nonvesicular routes (10). Based on our data and a recent report authored by Mesmin et al. (17), which showed that the genetic modulation of STARD4 expression in U2OS cells affects the movement of sterol at the ERC, we hypothesized that STARD4 would play a similar role in HepG2 cells under conditions of cholesterol deficiency. It has been previously shown that DHE, a naturally fluorescent cholesterol analog, mimics the characteristics of cholesterol in a variety of cells, is nontoxic, and equilibrates with the ERC within several minutes (27). Furthermore, the use of DHE to study ERC-cholesterol dynamics is a well-established technique (28–31). Using fluorescence recovery after photobleaching (FRAP), we examined the rate of DHE movement at the ERC.

We saw only a small difference in the rate and extent of DHE fluorescence recovery between D4 KD and control

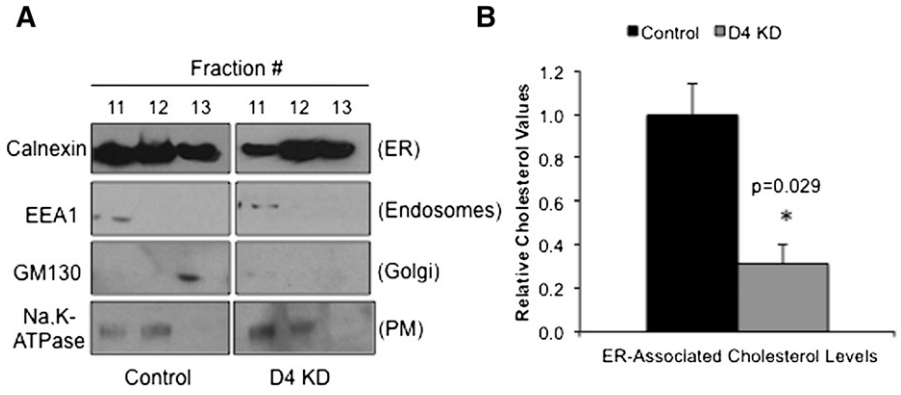

Fig. 5. ER-associated cholesterol levels are reduced in D4 KD cells. Control and D4 KD cells were subjected to subcellular fractionation using an Opti-Prep discontinuous gradient. A: Immunoblots of ER-specific fractions (no. 11–13). Fractions were tested for purity using antibody markers specific for the ER, endosomes, golgi, and PM. B: Total cholesterol values associated with ER-specific fractions (no. 11–13) normalized to total cellular protein.

cells under cholesterol poor conditions (**Fig. 6A**), with $T_{1/2}$ times of 118 s and 110 s, respectively. However, after 20 h in 5% LPDS, adding cholesterol back to the medium resulted in a 20% increase in DHE recovery at the ERC in control cells ($T_{1/2}$ = 94 s). This phenomenon did not occur in D4 KD cells, which displayed a similar $T_{1/2}$ to D4 KD cells under cholesterol-depleted conditions (117 s) (Fig. 6B).

To rule out a general alteration in endocytic recycling in the context STARD4 deficiency, we examined the level and distribution of the TfR as well as the recycling rates of its ligand Tf, and found no differences between control and D4 KD cells (**Fig. 7**). Thus, it appears that the ERC phenotype seen in D4 KD cells is a direct result of reduced STARD4 expression rather than defective endocytic recycling.

Compensatory responses to STARD4 deficiency in HepG2 cells

When there is a disruption in one or more components involved in maintaining intracellular cholesterol balance, cells respond accordingly. Given the potential overlap in function among intracellular cholesterol transport proteins, it is possible that our manipulation of STARD4 in D4 KD cells affects the expression pattern of other known cholesterol transporters.

To test this, we examined the protein expression of NPC1, SCP2, FABP1, OSBP, and STARD5 in control and D4 KD cells grown in either cholesterol-sufficient or cholesterol-poor conditions (**Fig. 8A**). The levels of all transporters remained unchanged, except for NPC1, which was reduced only under cholesterol deficiency in D4 KD cells.

In addition to compensatory responses via nonvesicular mechanisms, it is possible that vesicular cholesterol transport pathways also respond to reduced STARD4 levels in HepG2 cells. To test this, we examined the cellular status of the LDLR. There were no differences between cell lines regarding total LDLR levels; however, control and D4 KD cells exhibited slightly decreased total LDLR levels after cholesterol repletion relative to cholesterol-depleted conditions (Fig. 8B). Furthermore, biotin labeling indicated

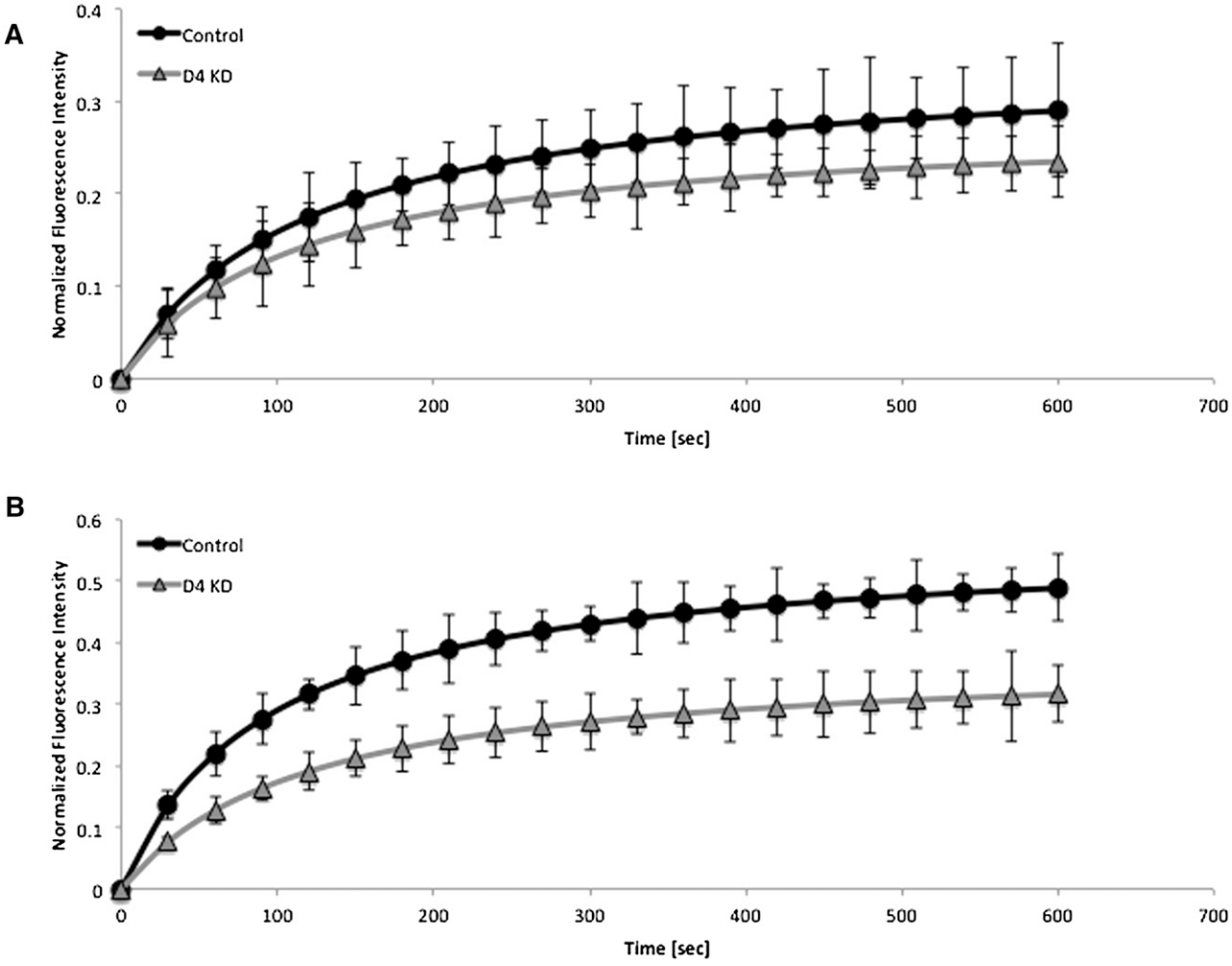

Fig. 6. Reduced rates of fluorescent recovery at the ERC in cholesterol-replete D4 KD cells. Control (circles) and D4 KD cells (triangles) were subjected to FRAP analysis as described in Materials and Methods. There were no immediate effects on DHE movement at the ERC after growth in cholesterol-poor conditions (A); however, after cholesterol repletion (B), D4 KD cells did not reach the fluorescent recovery levels of control cells, indicating a role for STARD4 at the ERC. $T_{1/2}$ times for cholesterol-depleted cells were 118.35 s (control) and 110.96 (D4 KD). $T_{1/2}$ times for cholesterol-loaded cells were 94.67 s (control) and 117.89 s (D4 KD). Results are representative of multiple replicates. Error bars represent SE.

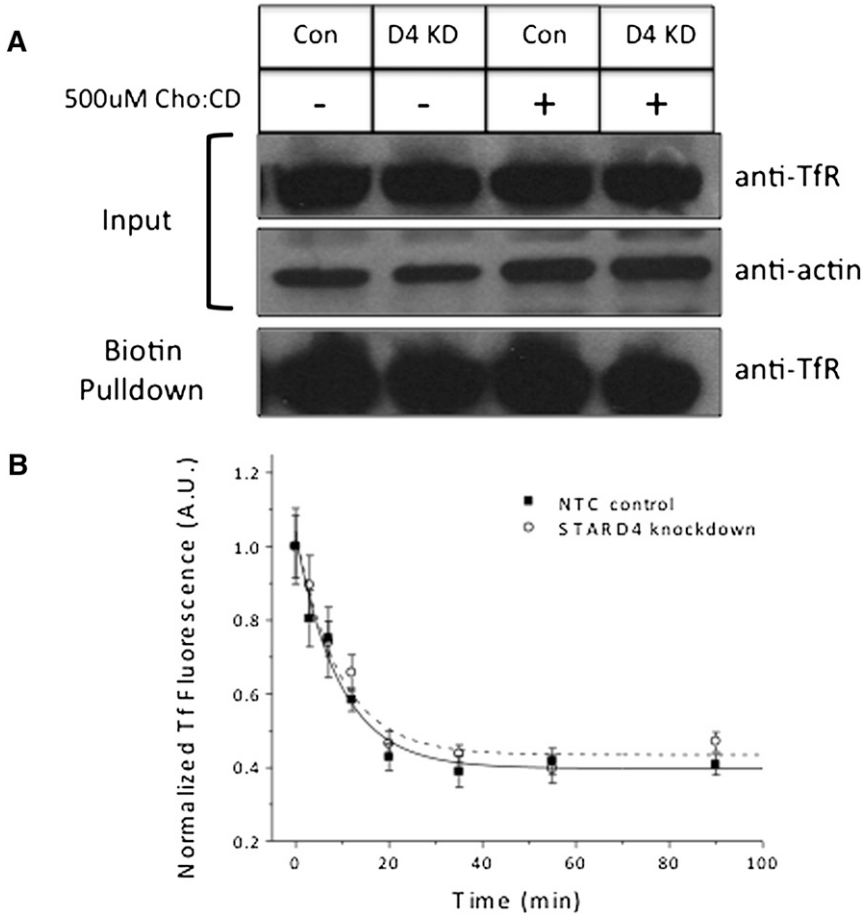

Fig. 7. TfR rate is unaffected in STARD4 knockdown HepG2. A: TfR kinetics were measured by fluorescence microscopy. B: The time course for Tf recycling is indistinguishable between STARD4 knockdown (circles, dashed line fit; $t_{1/2}$ = 6.4 ± 1.5 min) and control cells (squares, solid line fit; $t_{1/2}$ = 6.6 ± 1.1 min), suggesting that membrane trafficking from the plasma membrane through endosomal compartments is unaffected by the absence of STARD4. Error bars indicate SE of the mean cell intensity.

increased cell surface LDLR levels in D4 KD cells. Conversely, after cholesterol repletion, cell surface LDLR was decreased. These data suggest that the LDLR pathway might also compensate for reduced STARD4-mediated cholesterol transport.

DISCUSSION

STARD4, a member of the evolutionarily conserved START gene family, has been implicated in the nonvesicular intracellular transport of cholesterol, although the direction of transport and the membranes with which this protein interacts are not clear. We now present studies of STARD4 function using shRNA knockdown technology to reduce STARD4 expression in HepG2 cells. In this report, we provide evidence that STARD4 is associated with several cellular membranes (PM, ERC, and ER) and disruptions in STARD4 function affect the LDLR and NPC1 pathways, which likely represent compensatory responses.

To more precisely determine the functional role(s) of STARD4 in cells, we developed a model centered on reduced STARD4 expression. We performed these studies in the hepatocarcinoma cell line, HepG2, because in vivo STARD4 expression is highest in liver (22). Furthermore, the liver is central to cholesterol homeostasis.

Based on our previous work on STARD4 showing that it is regulated by the master cholesterol-sensing transcription factor SREBP2 (22), we hypothesized that conditions of cholesterol deficiency would induce STARD4 expression in normal HepG2 cells. To create an environment where cholesterol was scarce, we grew HepG2 cells in media containing 5% LPDS. This condition provided the largest observed differential in STARD4 expression (Fig. 1) and was the basis for all experiments described in this study.

Although there have been studies using siRNA to knockdown STARD4 expression in other cell types, such as osteosarcoma cells (17), we felt that HepG2 cells represented a more physiologically relevant system to examine STARD4 action. Therefore, we created a stable cell line of reduced STARD4 expression and grew these cells in 5% LPDS (along with their control counterparts) to give us the best chance to identify associated phenotypes.

Given the reported function of STARD4 as an intracellular cholesterol transport protein, we reasoned that intracellular cholesterol distribution would be affected in D4 KD cells. When using filipin fluorescent patterning as

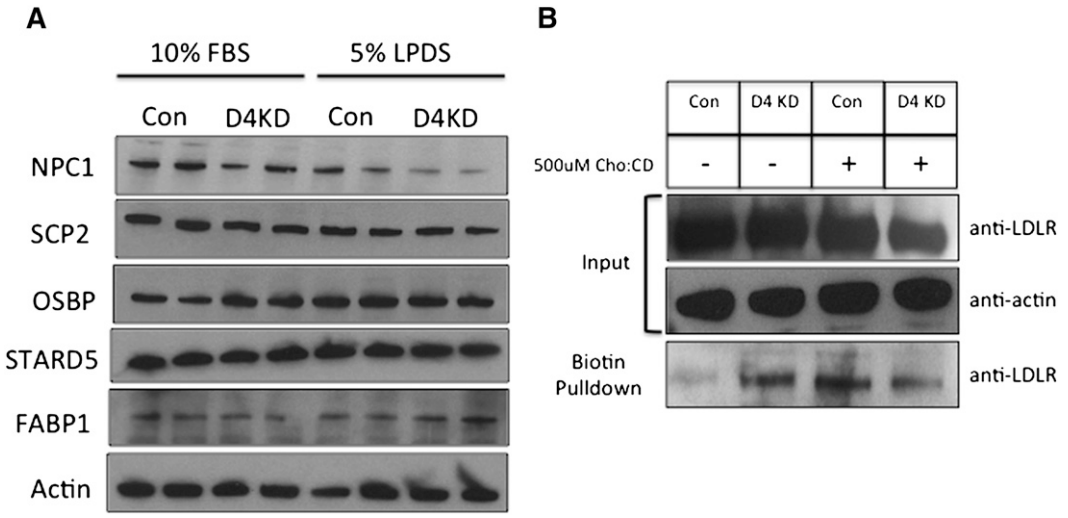

Fig. 8. Compensatory changes in the face of reduced STARD4 levels. Control and D4 KD cells were grown in cholesterol-poor or cholesterol-replete conditions, followed by an analysis of several intracellular cholesterol transport pathways. A: Western blot showing the protein expression of several intracellular cholesterol transport proteins in control and D4 KD cells. B: Biotinylation assay showing the level of LDLR at the cell surface.

a proxy for FC distribution, we did see an obvious increase in the level of FC retained at the PM in D4 KD cells, suggesting that STARD4 is involved in mobilizing the PM-cholesterol pool, particularly when exogenous cholesterol is limiting.

To expand on this finding, we set out to determine where the STARD4-mediated cholesterol mobilization from the PM was going within the cell. There are several lines of evidence pointing toward an interaction of STARD4 with the ER in a variety of cell types. For instance, Rodriguez-Agudo (14) reported in primary mouse hepatocytes that overexpression of STARD4 causes increased cellular CE formation by ACAT, presumably by delivering FC to the ER. More recently, this same group reported in THP-1 macrophages that STARD4 colocalizes to ACAT-rich areas of the ER and is associated with budding lipid droplets (18). Additionally, Mesmin reported decreased CE formation in cholesterol-loaded osteosarcoma cells treated with siRNA to reduce STARD4 levels (17).

By examining ACAT-mediated cholesterol esterification rates and measurements of total cholesterol in subcellular membrane fractions corresponding to the ER, we have shown that a reduction in STARD4 expression after growth in cholesterol-poor conditions also affects cholesterol transport to the ER. These data affirm an association of STARD4 with the ER and, together with our studies using filipin, suggest that STARD4 delivers FC from the PM to this organelle. However, there is additional evidence suggesting that STARD4 transports cholesterol between other cellular compartments. We have previously shown that the overexpression of STARD4 in COS1 cells cotransfected with plasmids encoding the cholesterol side-chain cleavage enzyme system increased cholesterol delivery to mitochondria, as evidenced by increased rates of steroidogenesis (22). Furthermore, Mesmin reported in osteosarcoma cells that overexpression of STARD4 increased DHE transport to the ER and the ERC (17). Because it has been shown that DHE is primarily transported from the PM to the ERC in a nonvesicular fashion (29), it is likely that STARD4 mediates this movement.

Using a liver cell model system, we have shown that STARD4 interacts with the ERC in HepG2 cells. Using FRAP analysis, we examined the rate of DHE movement into the ERC in control and D4 KD cells. Under cholesterol-poor conditions, the rate of DHE movement and the total fluorescence recovery were similar between control and D4 KD cells. However, after a short period of cholesterol repletion, control cells showed an increase in the rate and extent of sterol transport into the ERC, which was not seen in the D4 KD cells. Because D4 KD cells had normal rates of Tf recycling and normal levels of TfR at the cell surface, it is probable that STARD4 deficiency did not produce a generalized slow-down in endocytosis and vesicular transport to the ERC. Therefore, we conclude that these effects were related to defective STARD4-mediated nonvesicular trafficking to or away from the ERC.

Despite normal endocytic recycling, D4 KD cells exhibited a difference in the amount of the LDLR associated with the cell surface, as determined by biotinylation assays. More specifically, compared with controls, under cholesterol-poor conditions D4 KD cells had higher levels of cell surface LDLR. This situation was reversed after cholesterol repletion, and D4 KD cells had lower levels of cell surface LDLR compared with controls. Because total LDLR levels did not differ between D4 KD and control cells, this presumably represents a shift of LDLR to the cell surface to compensate for the deficiency of STARD4, thus allowing maintenance of cellular cholesterol homeostasis.

Given the relatively modest phenotype in the STARD4 knockout mouse (32), we were surprised to find a relatively consistent pattern of expression for several other intracellular cholesterol transport proteins, including STARD5, FABP1, SCP2, and OSBP. We did, however, observe a parallel between our mice and knockdown studies

regarding NPC1 expression. Here we report that NPC1 protein is decreased in D4 KD cells during cholesterol deficiency, which is consistent with the STARD4$^{-/-}$ mouse studies where a 2.5-fold decrease in NPC1 expression was observed. However, the expression of NPC1, which unidirectionally mobilizes cholesterol from late endosomes, does not respond to the amount of cholesterol flowing through cells (33). Therefore, the reduced NPC1 observed in the context of STARD4 deficiency likely arises as a result of secondary effects, perhaps involving altered signal transduction pathways.

In summary, these studies, our previous work, and the work of others have shown using in vitro model systems that STARD4 is capable of mediating the nonvesicular transport of cholesterol to or away from the PM, ERC, and ER. Further studies are needed to determine the exact contribution of STARD4 to cholesterol homeostasis in vivo.

The authors thank Dr. Edward Fisher (NYU Langone Medical Center, New York, NY) for the gift of the ACAT inhibitor F1394.

REFERENCES

1. Liscum, L., and N. Munn. 1999. Intracellular cholesterol transport. *Biochim. Biophys. Acta.* **1438:** 19–37.
2. Reinhart, M. P., J. T. Billheimer, J. R. Faust, and J. L. Gaylor. 1987. Subcellular localization of the enzymes of cholesterol biosynthesis and metabolism in rat liver. *J. Biol. Chem.* **262:** 9649–9655.
3. Haynes, M. P., M. Phillips, and G. Rothblat. 2000. Efflux of cholesterol from different cellular pools. *Biochemistry.* **39:** 4508–4517.
4. Zha, X., L. M. Pierini, P. L. Leopold, P. J. Skiba, I. Tabas, and F. R. Maxfield. 1998. Sphingomyelinase treatment induces ATP-independent endocytosis. *J. Cell Biol.* **140:** 39–47.
5. Skiba, P. J., X. Zha, F. Maxfield, S. Schissel, and I. Tabas. 1996. The distal pathway of lipoprotein-induced cholesterol esterification, but not sphingomyelinase-induced cholesterol esterification, is energy-dependent. *J. Biol. Chem.* **271:** 13392–13400.
6. Lavigne, P., R. Najmanivich, and J. G. Lehoux. 2010. Mammalian StAR-related lipid transfer (START) domains with specificity for cholesterol: structural conservation and mechanism of reversible binding. *Subcell. Biochem.* **51:** 425–437.
7. Soccio, R. E. 2003. StAR-related Lipid Transfer (START) proteins: mediators of intracellular lipid metabolism. *J. Biol. Chem.* **278:** 22183–22186.
8. Miller, W. 2007. Steroidogenic acute regulatory protein (StAR), a novel mitochondrial cholesterol transporter.*Biochim. Biophys. Acta.* **1771:** 663–676.
9. Maxfield, F. R., and A. K. Menon. 2006. Intracellular sterol transport and distribution. *Curr. Opin. Cell Biol.* **18:** 379–385.
10. Prinz, W. A. 2007. Non-vesicular sterol transport in cells. *Prog. Lipid Res.* **46:** 297–314.
11. Strauss, J. F, T. Kishida, L. Christenson, T. Fujimoto, and H. Hiroi. 2003. START domain proteins and the intracellular trafficking of cholesterol in steroidogenic cells. *Mol. Cell. Endocrinol.* **202:** 59–65.
12. Alpy, F. 2005. Give lipids a START: the StAR-related lipid transfer (START) domain in mammals. *J. Cell Sci.* **118:** 2791–2801.
13. Zhang, M., P. Liu, N. K. Dwyer, L. K. Christenson, T. Fujimoto, F. Martinez, M. Comly, J. A. Hanover, E. J. Blanchette-Mackie, and J. F. Strauss III. 2002. MLN64 mediates mobilization of lysosomal cholesterol to steroidogenic mitochondria. *J. Biol. Chem.* **277:** 33300–33310.
14. Rodriguez-Agudo, D., S. Ren, E. Wong, D. Marques, K. Redford, G. Gil, P. Hylemon, and W. M. Pandak. 2008. Intracellular cholesterol transporter StarD4 binds free cholesterol and increases cholesteryl ester formation. *J. Lipid Res.* **49:** 1409–1419.
15. Soccio, R. E., R. Adams, M. Romanowski, E. Sehayek, S. Burley, and J. Breslow. 2002. The cholesterol-regulated StarD4 gene encodes a StAR-related lipid transfer protein with two closely related homologues, StarD5 and StarD6. *Proc. Natl. Acad. Sci. USA.* **99:** 6943–6948.
16. Romanowski, M. J., R. Soccio, J. Breslow, and S. Burley. 2002. Crystal structure of the Mus musculus cholesterol-regulated START protein 4 (StarD4) containing a StAR-related lipid transfer domain. *Proc. Natl. Acad. Sci. USA.* **99:** 6949–6954.
17. Mesmin, B., N. H. Pipalia, F. W. Lund, T. F. Ramlall, A. Sokolov, D. Eliezer, et al. 2011. STARD4 abundance regulates sterol transport and sensing. *Mol. Biol. Cell.***22:** 4004–4015.
18. Rodriguez-Agudo, D., M. Calderon-Dominguez, S. Ren, D. Marques, K. Redford, M. A. Medina-Torres, et al. 2011. Subcellular localization and regulation of StarD4 protein in macrophages and fibroblasts. *Biochim. Biophys. Acta.* **1811:** 597–606.
19. Kruth, H. S. 1984. Histochemical detection of esterified cholesterol within human atherosclerotic lesions using the fluorescent probe filipin. *Atherosclerosis.* **51:** 281–292.
20. Yguerabide, J., J. A. Schmidt, and E. E. Yguerabide. 1982. Lateral mobility in membranes as detected by fluorescence recovery after photobleaching. *Biophys. J.* **40:** 69–75.
21. Tabas, I. Preparation of 14C-oleate-albumin solution for whole-cell cholesterol esterification assay. Accessed January 2009 at http://www.cumc.columbia.edu/dept/medicine/tabas_site/protocols/14C-oleate-albumin-1.htm
22. Soccio, R. E., R. Adams, K. Maxwell, and J. Breslow. 2005. Differential gene regulation of StarD4 and StarD5 cholesterol transfer proteins. Activation of StarD4 by sterol regulatory element-binding protein-2 and StarD5 by endoplasmic reticulum stress. *J. Biol. Chem.* **280:** 19410–19418.
23. Goldstein, J. L., and M. S. Brown. 1973. Familial hypercholesterolemia: identification of a defect in the regulation of 3-hydroxy-3-methylglutaryl coenzyme A reductase activity associated with overproduction of cholesterol. *Proc. Natl. Acad. Sci. USA.* **70:** 2804–2808.
24. Brown, M. S., S. E. Dana, and J. L. Goldstein. 1974. Regulation of 3-hydroxy-3-methylglutaryl coenzyme A reductase activity in cultured human fibroblasts. Comparison of cells from a normal subject and from a patient with homozygous familial hypercholesterolemia. *J. Biol. Chem.* **249:** 789–796.
25. Li, X., and M. Donowitz. 2008. Fractionation of subcellular membrane vesicles of epithelial and nonepithelial cells by OptiPrep density gradient ultracentrifugation. *Methods Mol. Biol.* **440:** 97–110.
26. Mukherjee, S., X. Zha, I. Tabas, and F. Maxfield. 1998. Cholesterol distribution in living cells: fluorescence imaging using dehydroergosterol as a fluorescent cholesterol analog. *Biophys. J.* **75:** 1915–1925.
27. Mesmin, B., and F. R. Maxfield. 2009. Intracellular sterol dynamics. *Biochim. Biophys. Acta.* **1791:** 636–645.
28. Wustner, D. 2007. Fluorescent sterols as tools in membrane biophysics and cell biology. *Chem. Phys. Lipids.* **146:** 1–25.
29. Hao, M., S. Lin, O. Karylowski, D. Wustner, T. McGraw, and F. Maxfield. 2002. Vesicular and non-vesicular sterol transport in living cells. The endocytic recycling compartment is a major sterol storage organelle. *J. Biol. Chem.* **277:** 609–617.
30. Mondal, M., B. Mesmin, S. Mukherjee, and F. R. Maxfield. 2009. Sterols are mainly in the cytoplasmic leaflet of the plasma membrane and the endocytic recycling compartment in CHO cells. *Mol. Biol. Cell.* **20:** 581–588.
31. Wustner, D., A. Herrmann, M. Hao, and F. Maxfield. 2002. Rapid nonvesicular transport of sterol between the plasma membrane domains of polarized hepatic cells. *J. Biol. Chem.* **277:** 30325–30336.
32. Riegelhaupt, J. J., M. P. Waase, J. Garbarino, D. E. Cruz, and J. L. Breslow. 2010. Targeted disruption of StARD4 leads to modest weight reduction and minor alterations in lipid metabolism. *J. Lipid Res.***51:** 1134–1143.
33. Garver, W. S., C. Xie, J. J. Repa, S. D. Turley, and J. M. Dietschy. 2005. Niemann-Pick C1 expression is not regulated by the amount of cholesterol flowing through cells in the mouse. *J. Lipid Res.* **46:** 1745–1754.